Spontaneous Exciton Dissociation in Carbon Nanotubes

Y. Kumamoto, M. Yoshida, A. Ishii, A. Yokoyama, T. Shimada, and Y. K. Kato*
Institute of Engineering Innovation, The University of Tokyo, Tokyo 113-8656, Japan
(Received 8 July 2013; published 17 March 2014)

Simultaneous photoluminescence and photocurrent measurements on individual single-walled carbon nanotubes reveal spontaneous dissociation of excitons into free electron-hole pairs. The correlation of luminescence intensity and photocurrent shows that a significant fraction of excitons are dissociating before recombination. Furthermore, the combination of optical and electrical signals also allows for extraction of the absorption cross section and the oscillator strength. Our observations explain the reasons why photoconductivity measurements in single-walled carbon nanotubes are straightforward despite the large exciton binding energies.

DOI: 10.1103/PhysRevLett.112.117401 PACS numbers: 78.67.Ch, 71.35.-y, 78.55.Kz, 78.56.-a

An enhancement of the Coulomb interaction occurs in one-dimensional systems because of limited screening [1], and single-walled carbon nanotubes (SWCNTs) are an ideal model system where such an effect manifests itself [2]. Electron-hole pairs form tightly bound excitons with a binding energy of a few hundred meV, which amounts to a significant fraction of the band-gap energy [3,4]. Such a large binding energy warrants the stability of excitons even at room temperature, and with exciton size being a few nm [5,6], strong fields on the order of 100 V/μm would be required for exciton dissociation [7].

In contrast to the expectation that the generation of free carriers from charge-neutral excitons would be difficult, photocurrent and photovoltaic measurements have proved to be simple and convenient tools for studying the properties of SWCNTs. Not only have they been used to measure potential landscapes [8–11], optical absorption properties [12–14], and ultrafast carrier dynamics [15], they have been instrumental in investigating unique effects that occur in SWCNTs, such as band-gap renormalization [16] and multiple electron-hole pair generation [17]. It has been a perplexing situation where exciton dissociation has not been brought up as an obstacle for performing these experiments. In interpreting the results, quantitative discussion on the dissociation process has been scarce, and in some cases the excitonic effects have not been considered at all.

Here we resolve such an inconsistency by performing simultaneous photoluminescence (PL) and photocurrent (PC) measurements on individual SWCNTs. Nonzero photoconductivity is observed even at small fields, indicating that excitons are spontaneously dissociating. A simple model is constructed to consistently describe the excitation power and voltage dependencies of the PL and PC. Using this model, we find that a good fraction, if not a majority, of excitons are dissociating into free carriers. Within the same analysis framework, we are also able to extract the absorption cross section and the oscillator strength at the E_{22} resonance.

Our devices are field-effect transistors with individual air-suspended SWCNTs [18] as shown in Fig. 1(a). We start with a Si substrate with 1 μm-thick oxide, and etch $\sim$500 nm-deep trenches into the oxide layer. An electron beam evaporator is used to deposit 3 nm Ti and 45 nm Pt for electrodes. Finally, catalyst particles are placed on the contacts and alcohol chemical vapor deposition is performed to grow SWCNTs [19,20]. A scanning electron micrograph of a typical device is shown in Fig. 1(b).

We look for devices that show nanotube PL at the trench in between the electrodes using a confocal microscope [21,22]. A continuous-wave Ti:sapphire laser is used for excitation and PL is detected by an InGaAs photodiode array attached to a spectrometer. The PC measurements are performed by monitoring the current through the device in the presence of a bias voltage V. We apply $-V/2$ and $+V/2$ to the two contacts, respectively, and ground the Si substrate. Although we do not expect much electrostatic doping because of the relatively thick oxide, this configuration ensures that the effective gate voltage at the center of the trench is zero. The current is averaged while a PL spectrum is collected, and the PC is obtained by subtracting the dark current measured in a similar manner with the laser blocked by a shutter. All measurements are done in air at room temperature.

Figure 1(c) is an optical microscope image of the device, and in the area indicated by the black box, we perform reflectivity, PL, and PC imaging simultaneously at an excitation laser power $P = 15$ μW. The reflectivity image [Fig. 1(d)] shows the position of the trench, and a luminescent nanotube suspended over the trench can be seen in the PL image [Fig. 1(e)]. The PC image shows that the signal is maximized at the same spot as PL [Fig. 1(f)]. In contrast to the case of Schottky barrier imaging [8–11], we do not observe PC when the laser spot is near or on the contacts. This confirms that band bending and electrostatic doping near the contacts are negligible in our voltage configuration.

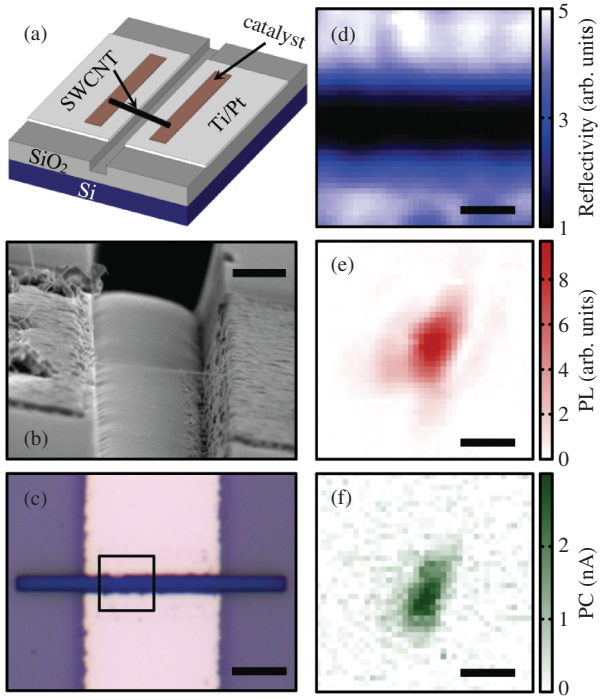

FIG. 1 (color). (a) A schematic of a device. (b) A scanning electron micrograph of a typical device. (c) A top-view optical microscope image of a device with a trench width of 1.3 μm. The black box shows the scan area for imaging measurements shown in (d)–(f). The scale bars in (b) and (c) are 0.5 μm and 4 μm, respectively. (d), (e), and (f) are reflectivity, PL, and PC images, respectively. The scale bars are 1 μm. Excitation energy and bias voltage are 1.651 eV and 20 V, respectively, and laser polarization angle is adjusted to maximize the PL signal. For (e), the PL image is extracted at an emission energy of 922 meV with a spectral integration window of 7 meV.

PL excitation spectroscopy performed on this nanotube at zero bias voltage shows a clear single peak [Fig. 2(a)], and we identify the nanotube chirality to be (10, 6). By performing such an excitation spectroscopy under an application of bias, we obtain PL and PC excitation spectra simultaneously [Fig. 2(b)]. Both PL and PC have a peak at the same excitation energy corresponding to the E_{22} resonance. The spatial and spectral coincidence of the PL and PC signals show that both are indeed coming from the same nanotube.

On this device, the excitation power and bias voltage dependencies are investigated in Figs. 3(a)–3(d). We first discuss the excitation power dependence. For all of the voltages, the PC signal shows a linear increase with excitation power [Fig. 3(a)], whereas PL shows a sublinear increase [Fig. 3(b)]. The latter behavior is known to be caused by exciton-exciton annihilation [21,23–25]. If the observed PC is caused by dissociation of the E_{11} excitons, then we expect PC to scale with PL, as both of the signals should be proportional to the number of E_{11} excitons.

Rather, the linear behavior suggests that the PC is proportional to the number of excitons injected at the

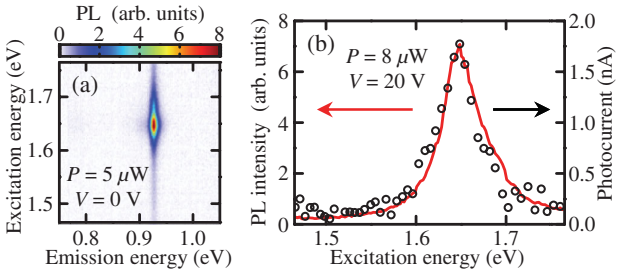

FIG. 2 (color). (a) A PL excitation map for the same nanotube as shown in Figs. 1(d)–(f) for $P = 5$ μW and $V = 0$ V. (b) PL (red curve) and PC (open circles) spectra taken with $P = 8$ μW and $V = 20$ V. Laser polarization is parallel to the nanotube axis. PL intensity is obtained by fitting the emission spectra with Lorentzian functions and taking the peak area.

E_{22} energy, and that dissociation of E_{11} excitons is negligible. There are at least two different processes that can result in the dissociation of E_{22} excitons. It is possible that the applied electric field induces the dissociation, and in this case one would expect some threshold voltage at which the dissociation occurs [7]. Another conceivable scenario is the dissociation that happens spontaneously in the course of relaxation down to E_{11} exciton states.

The two pictures can be distinguished by examining the voltage dependence of the PC [Fig. 3(c)]. We observe that the PC has a slightly superlinear dependence on the applied voltage, but there exists some slope near $V = 0$. This implies that the conductivity is nonzero even at zero applied bias, supporting the interpretation that the injected excitons are spontaneously dissociating. Those carriers that are swept into the contacts before binding into E_{11} excitons would generate the PC.

We note that the lack of field-induced dissociation for E_{22} excitons is consistent with the interpretation of the intensity dependencies that E_{11} exciton dissociation is negligible. The binding energy for E_{22} excitons is larger than E_{11} excitons [26], and therefore we do not expect field-induced dissociation of E_{22} excitons if E_{11} excitons are still intact. Measurements with an excitation at the E_{12} resonance do not show much change in PL intensity with voltage [27], also suggesting that field-induced dissociation is not important at these fields.

As the continuum for E_{11} excitons lies below E_{22}, it may seem reasonable to attribute the spontaneous dissociation to direct electronic transition to free electron-hole pairs. It has been suggested, however, that such a process is much weaker than phonon-mediated relaxation to E_{11} and E_{12} exciton states [28]. Since relaxation to excitonic states does not result in free carriers, we speculate that dissociation involving a free electron-hole pair with an emission of a phonon may be responsible for the observed photocurrent. Another possible mechanism is the free-carrier generation from E_{11} exciton-exciton annihilation [29]. As the

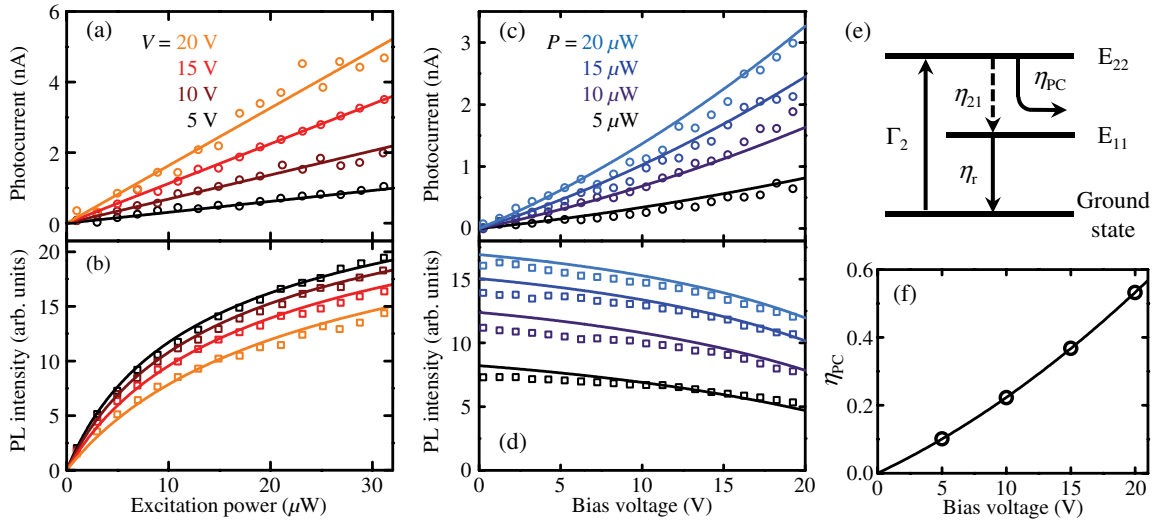

FIG. 3 (color online). (a) Excitation power dependence of PC. Data from bottom to top correspond to $V = 5$, 10, 15, and 20 V. (b) Power dependence of PL, with data from top to bottom corresponding to $V = 5$, 10, 15, and 20 V. (c) and (d) Bias voltage dependence of PC and PL, respectively. Data from bottom to top correspond to $P = 5$, 10, 15, and 20 μW. For (a)–(d), the same tube as shown in Figs. 1(d)–(f) was measured with the laser spot at the center of the nanotube. The excitation energy is fixed at 1.651 eV and the laser polarization is parallel to the nanotube axis. Symbols are data and lines are simulation results as explained in the text. (e) A schematic of the model used to produce the curves shown in (a)–(d). (f) η_{PC} as a function of V. Open circles are data obtained from (b) and the line is a fit as explained in the text.

annihilation process is extremely efficient for air-suspended nanotubes [21,25], it may explain the existence of free carriers. It is not clear why we do not observe trion emission as in the case of micelle-encapsulated nanotubes [29].

The voltage dependence of the PL [Fig. 3(d)] shows a decrease of PL with increasing voltage. Different from the case where no PC flows [30], we expect that less excitons relax into E_{11} at higher voltages as photocarriers are extracted into the contacts. As the current gives the absolute rate of electron-hole pairs extracted from the nanotube, we can deduce the number of excitons removed from the system. By modeling such a fractioning in the exciton population, we are able to determine the number of injected excitons, and in turn the absorption cross section.

Figure 3(e) shows a schematic of our model. E_{22} excitons are generated at a rate

$$\Gamma_2 = \int n\sigma \frac{2P}{\pi r^2 E} \exp\left(-2\frac{x^2}{r^2}\right) dx = \sqrt{\frac{2}{\pi}} \frac{n}{rE} \sigma P, \qquad (1)$$

where $n = 130$ nm^{-1} is the number of atoms per length, σ is the absorption cross section per carbon atom, $r = 492$ nm is the $1/e^2$ radius of the laser spot, and E is the laser photon energy. The fraction of the excitons that are extracted by PC is denoted by η_{PC}, while $\eta_{21} = 1 - \eta_{PC}$ represents the fraction that relax down to the E_{11} sublevel. The fraction of the E_{11} excitons that recombine radiatively and contribute to PL is represented by a nonlinear function $\eta_r(\Gamma_1)$ which includes the effects of exciton-exciton annihilation. Here, $\Gamma_1 = \Gamma_2 \eta_{21}$ is the rate at which the E_{11} excitons are populated.

The absolute values of η_{21} can be obtained from the excitation-power dependence of PL [Fig. 3(b)]. At $V = 0$, there are no PC and therefore $\eta_{PC} = 0$ and $\eta_{21} = 1$. When voltages are applied, Γ_1 decreases by a factor η_{21}. By scaling the excitation power to match the dependence at $V = 0$, the values of η_{21} are obtained for the four voltages. We plot $\eta_{PC} = 1 - \eta_{21}$ in Fig. 3(f).

Having obtained the explicit values of η_{PC}, we can now determine σ. Within our model, the PC is given by

$$I = e\eta_{PC}\Gamma_2 = \sqrt{\frac{2}{\pi}} \frac{e\eta_{PC} n}{rE} \sigma P, \qquad (2)$$

where e is the electron charge, and the only unknown parameter is σ. We find that a value of $\sigma = 2.4 \times 10^{-17}$ cm^2 best matches the PC data in Fig. 3(a). This value is comparable to recent measurements of σ at the E_{22} resonance in micelle-encapsulated tubes [31] and on-substrate tubes [32].

In addition to σ, the oscillator strength f is obtained using its relation to the integrated absorption cross section [33]. We fit the E_{22} resonance with a Lorentzian profile and obtain a linewidth of $\hbar\gamma = 44.5$ meV, where $\hbar$ is the Planck constant, and we use $f = \epsilon_0 mc\sigma\gamma/e^2$, where ϵ_0 is the vacuum permittivity, m is the electron mass, and c is the speed of light. We find $f = 0.015$, which is somewhat larger compared to (6,5) nanotubes [6].

TABLE I. Absorption cross section and oscillator strength for the eight nanotubes measured. Lorentzian fits to PL excitation spectra at $V = 0$ V are used to obtain the E_{22} energy and full width at half-maximum $\hbar\gamma$.

Chirality	E_{22} (eV)	$\hbar\gamma$ (meV)	σ ($\times 10^{-17}$ cm^2)	f
(8,7)	1.724	66.6	2.1	0.020
(8,7)	1.712	58.4	2.6	0.022
(8,7)	1.717	71.3	1.7	0.017
(8,7)	1.725	69.1	2.5	0.025
(9,7)	1.593	44.2	9.5	0.060
(9,8)	1.555	50.5	7.1	0.052
(10,6)	1.652	44.5	2.4	0.015
(10,8)	1.452	51.5	1.3	0.009

To verify the validity of our model, we simulate the intensity and voltage dependencies of PC and PL using the parameters obtained above. For the voltage dependence of η_{PC}, we fit the data in Fig. 3(f) with a linear term and a quadratic term. We use an analytic expression derived in Ref. [24] for the form of $\eta_r(\Gamma_1)$, with the parameters adjusted to fit our data. As shown as solid lines in Figs. 3(a)–(d), the model consistently explains all the data simultaneously.

The behavior of η_{PC} shows that a large fraction of the injected excitons are dissociating, reaching a value as high as $\eta_{\mathrm{PC}} = 0.53$ at $V = 20$ V. We expect PC to saturate above a certain voltage when all free carriers are extracted, but we do not see any signs of such saturation. This suggests that there are much more free carriers available even at the highest bias voltage we used, implying that the majority of the injected excitons are dissociating.

In order to check the reproducibility and to obtain σ for other chiralities, we have performed similar measurements on other devices and the results are summarized in Table I. For four tubes with a chirality of (8,7), we find that f falls within $\pm 20\%$ and that the values are close to the theoretical estimate of $(0.014\ \mathrm{eV}^{-1})E_{22} = 0.024$ [26]. We have observed that σ can differ by a factor of 3 or so for other chiralities, but additional measurements should be performed as these are based on single devices for each chirality.

We note that our model does not consider any direct recombination of E_{22} excitons, which occurs prior to relaxation to the E_{11} state—for example, exciton-exciton annihilation at the E_{22} level [34]. Such a process would lead to an underestimate of the number of injected excitons, and σ would be larger than what we have deduced from our model. We also do not take into account any field-induced changes to η_r, but further measurements at different excitation energies are expected to clarify the contribution of such effects.

In summary, we have performed simultaneous PL and PC spectroscopy on individual SWCNTs and constructed a model that consistently explains the excitation power and voltage dependencies. Within the voltage range explored, we did not find evidences of field-induced exciton dissociation, for either of the E_{11} and E_{22} excitons. Instead, a considerable fraction of the injected excitons are found to spontaneously dissociate into free electron-hole pairs. We have also obtained the absorption cross section and the oscillator strength from these air-suspended SWCNTs. Our findings explain why the large exciton binding energies do not impede photoconductivity measurements in SWCNTs.

We thank R. Saito, Y. Miyauchi, and S. Maruyama for helpful discussions, T. Kan and I. Shimoyama for the use of the evaporator, S. Chiashi and S. Maruyama for the electron microscope, and S. Yamamoto for the plasma etcher. This work is supported by KAKENHI (21684016, 23104704, 24340066, 24654084), SCOPE, and KDDI Foundation, as well as the Photon Frontier Network Program of MEXT, Japan. The devices were fabricated at the Center for Nano Lithography & Analysis at The University of Tokyo.

*Corresponding author.
ykato@sogo.t.u-tokyo.ac.jp

[1] T. Ogawa and T. Takagahara, Phys. Rev. B **44**, 8138 (1991).
[2] T. Ando, J. Phys. Soc. Jpn. **66**, 1066 (1997).
[3] F. Wang, G. Dukovic, L. E. Brus, and T. F. Heinz, Science **308**, 838 (2005).
[4] J. Maultzsch, R. Pomraenke, S. Reich, E. Chang, D. Prezzi, A. Ruini, E. Molinari, M. S. Strano, C. Thomsen, and C. Lienau, Phys. Rev. B **72**, 241402(R) (2005).
[5] L. Lüer, S. Hoseinkhani, D. Polli, J. Crochet, T. Hertel, and G. Lanzani, Nat. Phys. **5**, 54 (2009).
[6] F. Schöppler, C. Mann, T. C. Hain, F. M. Neubauer, G. Privitera, F. Bonaccorso, D. Chu, A. C. Ferrari, and T. Hertel, J. Phys. Chem. C **115**, 14682 (2011).
[7] V. Perebeinos and P. Avouris, Nano Lett. **7**, 609 (2007).
[8] K. Balasubramanian, M. Burghard, K. Kern, M. Scolari, and A. Mews, Nano Lett. **5**, 507 (2005).
[9] M. Freitag, J. C. Tsang, A. Bol, P. Avouris, D. Yuan, and J. Liu, Appl. Phys. Lett. **91**, 031101 (2007).
[10] Y. H. Ahn, A. W. Tsen, B. Kim, Y. W. Park, and J. Park, Nano Lett. **7**, 3320 (2007).
[11] N. Rauhut, M. Engel, M. Steiner, R. Krupke, P. Avouris, and A. Hartschuh, ACS Nano **6**, 6416 (2012).
[12] J. U. Lee, P. J. Codella, and M. Pietrzykowski, Appl. Phys. Lett. **90**, 053103 (2007).
[13] A. D. Mohite, P. Gopinath, H. M. Shah, and B. W. Alphenaar, Nano Lett. **8**, 142 (2008).
[14] M. Barkelid, G. A. Steele, and V. Zwiller, Nano Lett. **12**, 5649 (2012).
[15] L. Prechtel, L. Song, S. Manus, D. Schuh, W. Wegscheider, and A. W. Holleitner, Nano Lett. **11**, 269 (2011).
[16] J. U. Lee, Phys. Rev. B **75**, 075409 (2007).
[17] N. M. Gabor, Z. Zhong, K. Bosnick, J. Park, and P. L. McEuen, Science **325**, 1367 (2009).
[18] S. Yasukochi, T. Murai, S. Moritsubo, T. Shimada, S. Chiashi, S. Maruyama, and Y. K. Kato, Phys. Rev. B **84**, 121409(R) (2011).
[19] S. Maruyama, R. Kojima, Y. Miyauchi, S. Chiashi, and M. Kohno, Chem. Phys. Lett. **360**, 229 (2002).

[20] S. Imamura, R. Watahiki, R. Miura, T. Shimada, and Y. K. Kato, Appl. Phys. Lett. **102**, 161102 (2013).
[21] S. Moritsubo, T. Murai, T. Shimada, Y. Murakami, S. Chiashi, S. Maruyama, and Y. K. Kato, Phys. Rev. Lett. **104**, 247402 (2010).
[22] R. Watahiki, T. Shimada, P. Zhao, S. Chiashi, S. Iwamoto, Y. Arakawa, S. Maruyama, and Y. K. Kato, Appl. Phys. Lett. **101**, 141124 (2012).
[23] K. Matsuda, T. Inoue, Y. Murakami, S. Maruyama, and Y. Kanemitsu, Phys. Rev. B **77**, 033406 (2008).
[24] Y. Murakami and J. Kono, Phys. Rev. B **80**, 035432 (2009).
[25] Y.-F. Xiao, T. Q. Nhan, M. W. B. Wilson, and J. M. Fraser, Phys. Rev. Lett. **104**, 017401 (2010).
[26] V. Perebeinos, J. Tersoff, and P. Avouris, Phys. Rev. Lett. **92**, 257402 (2004).
[27] See Supplemental Material at http://link.aps.org/supplemental/10.1103/PhysRevLett.112.117401 for the voltage dependence of PL with an E_{12} excitation.
[28] T. Hertel, V. Perebeinos, J. Crochet, K. Arnold, M. Kappes, and P. Avouris, Nano Lett. **8**, 87 (2008).
[29] S. M. Santos, B. Yuma, S. Berciaud, J. Shaver, M. Gallart, P. Gilliot, L. Cognet, and B. Lounis, Phys. Rev. Lett. **107**, 187401 (2011).
[30] A. V. Naumov, S. M. Bachilo, D. A. Tsyboulski, and R. B. Weisman, Nano Lett. **8**, 1527 (2008).
[31] L. Oudjedi, A. N. G. Parra-Vasquez, A. G. Godin, L. Cognet, and B. Lounis, J. Phys. Chem. Lett. **4**, 1460 (2013).
[32] D. Y. Joh, J. Kinder, L. H. Herman, S.-Y. Ju, M. A. Segal, J. N. Johnson, G. K.-L. Chan, and J. Park, Nat. Nanotechnol. **6**, 51 (2011).
[33] J. J. Sakurai and J. Napolitano, *Modern Quantum Mechanics*, (Addison-Wesley, San Francisco, 2011) 2nd ed.
[34] D. M. Harrah, J. R. Schneck, A. A. Green, M. C. Hersam, L. D. Ziegler, and A. K. Swan, ACS Nano **5**, 9898 (2011).